

SSMTL++: Revisiting Self-Supervised Multi-Task Learning for Video Anomaly Detection

Antonio Barbalau¹, Radu Tudor Ionescu^{1,2,*}, Mariana-Iuliana Georgescu^{1,2},
Jacob Dueholm^{3,4}, Bharathkumar Ramachandra⁵, Kamal Nasrollahi^{3,4},
Fahad Shahbaz Khan^{6,7}, Thomas B. Moeslund³, Mubarak Shah⁸

¹University of Bucharest, Romania, ²SecurifAI, Romania, ³Aalborg University, Denmark,
⁴Milestone Systems, Denmark, ⁵Geopipe Inc, US, ⁶MBZ University of Artificial Intelligence, UAE,
⁷Linköping University, Sweden, ⁸University of Central Florida, US

Abstract

A self-supervised multi-task learning (SSMTL) framework for video anomaly detection was recently introduced in literature. Due to its highly accurate results, the method attracted the attention of many researchers. In this work, we revisit the self-supervised multi-task learning framework, proposing several updates to the original method. First, we study various detection methods, e.g. based on detecting high-motion regions using optical flow or background subtraction, since we believe the currently used pre-trained YOLOv3 is suboptimal, e.g. objects in motion or objects from unknown classes are never detected. Second, we modernize the 3D convolutional backbone by introducing multi-head self-attention modules, inspired by the recent success of vision transformers. As such, we alternatively introduce both 2D and 3D convolutional vision transformer (CvT) blocks. Third, in our attempt to further improve the model, we study additional self-supervised learning tasks, such as predicting segmentation maps through knowledge distillation, solving jigsaw puzzles, estimating body pose through knowledge distillation, predicting masked regions (inpainting), and adversarial learning with pseudo-anomalies. We conduct experiments to assess the performance impact of the introduced changes. Upon finding more promising configurations of the framework, dubbed SSMTL++v1 and SSMTL++v2, we extend our preliminary experiments to more data sets, demonstrating that our performance gains are consistent across all data sets. In most cases, our results on Avenue, ShanghaiTech and UBnormal raise the state-of-the-art performance to a new level.

1. Introduction

Due its applicability in video surveillance, anomaly detection is an actively studied topic in the video domain, with many recent attempts trying to solve the problem by employing various approaches ranging from outlier detection

models [2, 8, 9, 11, 15, 21, 29, 32, 35, 37, 40, 43, 45, 47, 48, 52, 54, 55, 56, 58, 59, 61, 64, 69, 75, 78, 87, 85, 86] and weakly-supervised learning frameworks [16, 53, 67, 70, 83, 88] to supervised open-set methods [1]. Despite the numerous attempts in solving the problem, video anomaly detection remains a challenging task, especially due to the fact that abnormal events are determined by the context. For example, a pedestrian walking on the sidewalk is a normal event, but a pedestrian who crosses the street far from a crosswalk is an abnormal event (in some countries, pedestrians can even get fines for crossing the street in forbidden areas). Furthermore, since abnormal events are typically rare, it is difficult to collect training data to build fully supervised models. This adds to the difficulty of solving the task. Hence, more research efforts are required towards solving video anomaly detection. Perhaps one of the most promising directions in video anomaly detection without anomalies at training time is to address the task by learning a self-supervised framework on multiple proxy tasks, which are correlated to anomaly detection, as proposed by Georgescu *et al.* [18]. Indeed, Georgescu *et al.* [18] introduced a self-supervised multi-task learning (SSMTL) method that learns a set of four proxy tasks using a single 3D convolutional backbone with multiple heads (one head per task), obtaining state-of-the-art performance levels.

Although the SSMTL model attains very good results, we consider that the framework has a very high potential of obtaining even better results, which can be unearthed by studying and evaluating component variations in depth. To this end, we revisit the self-supervised multi-task learning framework [18], proposing several updates that boost the performance of the method, especially when we combine these updates and generate new frameworks, which we term SSMTL++v1 and SSMTL++v2. We identified three important components worth revisiting, namely the object detection method, the multi-task learning backbone architecture, and the proxy tasks. First, we study additional detection methods, e.g. based on detecting high-motion regions us-

*corresponding author: raducu.ionescu@gmail.com

ing optical flow or background subtraction, since we conjecture the currently used pre-trained YOLOv3 is suboptimal, *e.g.* objects in motion or objects from unknown classes are never detected. Next, we modernize the 3D convolutional backbone by introducing multi-head self-attention modules, inspired by the recent success of vision transformers [6, 14, 74]. As such, we alternatively introduce both 2D and 3D convolutional vision transformer (CvT) blocks [74]. Finally, we study additional proxy tasks, such as predicting segmentation maps through knowledge distillation, solving jigsaw puzzles, estimating body pose through knowledge distillation, predicting masked regions (inpainting), and adversarial learning with pseudo-anomalies.

We perform preliminary experiments to determine the impact of introducing the novel components into the SSMTL framework. Through the preliminary experiments, we find two novel and promising combinations (SSMTL++v1 and SSMTL++v2). We evaluate our new frameworks on three benchmark data sets: Avenue [43], ShanghaiTech [45] and UBnormal [1]. We report considerable performance gains with respect to SSMTL [18], while also attaining superior results compared to other recent state-of-the-art methods [4, 5, 6, 7, 11, 12, 13, 19, 20, 27, 29, 30, 35, 36, 38, 42, 44, 46, 49, 51, 52, 54, 55, 62, 67, 68, 72, 73, 75, 79, 80, 81, 82, 84].

In summary, our contribution is threefold:

- We introduce additional detection methods into SSMTL to increase the number of detected objects, providing empirical evidence to showcase the benefit of each detection method.
- We introduce convolutional vision transformer blocks into the backbone architecture, reporting performance improvements with our stronger backbone.
- We study various proxy tasks to be included into the SSMTL framework, finding novel task combinations that produce superior performance levels.

2. Related Work

Video anomaly detection. One dimension of taxonomy divides video anomaly detection methods into those that address single-scene and multi-scene problem formulations. Under this classification, the self-supervised multi-task learning framework treats the multi-scene formulation of the problem, where the training set may contain videos from multiple scenes and anomalies are not expected to be location-dependant. Another dimension categorizes methods into distance-based [27, 55, 56, 58, 65, 66, 71, 77], probabilistic [2, 8, 17, 26, 32, 48, 76], reconstruction-based [20, 21, 45, 49, 52, 59, 62, 72] and change detection [10, 28, 41] approaches. As SSMTL is based on multiple self-supervised tasks, it is not possible to place it into only one of these categories. For example, due to the *middle bounding box prediction* task, SSMTL can be viewed as a

reconstruction-based approach, where the basic premise is to train a model that reconstructs normal data with higher fidelity as compared to abnormal data, and some composite measure of reconstruction error subsequently acts as the anomaly score. Similar to several other methods in video anomaly detection [8, 17, 26, 27, 56, 72], SSMTL operates at the object patch level as opposed to at the frame level, but is one of the few reconstruction-based methods to do so ([45]). For an extensive treatment of taxonomy in video anomaly detection, we refer the reader to [57].

Certainly, we consider SSMTL [18] the closest method to the approaches presented in this paper, namely SSMTL++v1 and SSMTL++v2. We underline that the contributions presented in Section 1 also represent the differences with respect to the most related method.

Multi-task learning. As computing devices get faster, more specialized for deep learning applications and have more memory, multi-task learning approaches have started gaining popularity, such as with Mask-RCNN [24] for object detection and instance segmentation. The basic underlying premise of multi-task approaches is that learning to solve multiple tasks relevant to a primary (target) task is beneficial. When dealing with a problem such as video anomaly detection, where anomalous data is not provided at training time, the primary task cannot be directly supervised; herein lies the motivation for using multi-task learning. Multi-task approaches to video anomaly detection have been used sparsely before [52, 69]. However, to the best of our knowledge, SSMTL is the first to propose multi-task learning explicitly and intentionally for generalizing better to the out-of-distribution anomalous patterns in video. Certainly, our approaches are based on the same principle.

Self-supervised learning. Self-supervised learning is garnering traction with recent advances showing that, under the right conditions, self-supervised pre-training can outperform fully supervised pre-training in terms of transfer performance in downstream tasks [22, 23]. Self-supervised learning has been widely used before for video anomaly detection. Most reconstruction-based approaches use some form of self-supervised learning. The major approaches include frame-level reconstruction [21], future frame prediction [11, 39] or middle frame prediction [35]. The SSMTL framework however is the first to use middle patch prediction at the object level.

3. Method

Original framework. Georgescu *et al.* [18] proposed SSMTL, an object-centric framework based on self-supervised and multi-task learning on four proxy tasks. Indeed, the proposed model is trained on three self-supervised tasks and one knowledge distillation task. The whole architecture is composed of a shared 3D CNN backbone and four independent prediction or reconstruction heads (one

per proxy task). The last layer of the shared 3D CNN is global temporal pooling. Therefore, the prediction heads can use 2D convolutions.

The first step of the SSMTL framework is to obtain the object bounding boxes using the YOLOv3 [60] object detector. For each object in the frame i , a so-called *object-centric temporal sequence* is created by cropping the corresponding bounding box from the frames $\{i - t, \dots, i - 1, i, i + 1, \dots, i + t\}$. The *object-centric temporal sequence* is used as input to the 3D CNN.

The first proxy task (\mathbf{T}_1) is *predicting the arrow of time*, where the model learns to predict if the temporal sequence is moving forward or backward in time. The second proxy task (\mathbf{T}_2) is *predicting motion irregularity*, where the model is trained to predict if the object-centric temporal sequence is cropped from consecutive or intermittent frames, *i.e.* some frames are skipped in the forward direction to create irregular motion. The third self-supervised proxy task (\mathbf{T}_3) is *middle bounding box prediction*, where the middle crop (the bounding box cropped from the frame i) is deleted from the temporal sequence and the model is trained to predict the content of the missing bounding box. The fourth proxy task (\mathbf{T}_4) is *model distillation*. Here, the model is trained to predict the pre-softmax features of a pre-trained ResNet-50 [25] and the class probabilities predicted by the YOLOv3 [60] object detector.

The model is jointly optimized on all four proxy tasks. During inference, the object detector is applied on each frame. Then, for each detected object, the object-centric temporal sequence is created. The temporal sequence is passed through the CNN model, obtaining the output of each prediction head. For T_1 , the probability that the temporal sequence is moving backward is interpreted as the anomaly score. Similarly, the probability of the temporal sequence to be intermittent is considered as the anomaly score for T_2 . For T_3 , the anomaly score is computed as the mean absolute difference between the reconstruction of the middle bounding box predicted by the model and the ground-truth middle bounding box. For T_4 , only the absolute difference between the class probabilities predicted by the YOLOv3 object detector and those predicted by the model are taken into consideration, saving the time need to run ResNet-50 during inference. The anomaly score for each object is computed as the average of the anomaly scores given by each prediction head.

Updates overview. We identified three main components that are promising candidates for receiving updates that could positively impact the performance of SSMTL. The first component is the object detection method, which is currently based on a single pre-trained object detector. Increasing the number of detected objects is likely to increase the number of detected anomalies. Hence, we consider adding more detection methods. The second component is the

shared backbone architecture. Here, we propose and evaluate two different ways of integrating transformer blocks, which could strengthen the learning capacity of the framework. The last component worth investigating is the set of proxy tasks. Georgescu *et al.* [18] showed that the four proxy tasks employed in the original SSMTL framework are useful, but we believe that there are many other proxy tasks that could prove beneficial. We present our updates to these three components in separate sections below.

3.1. Introducing New Detection Methods

The object detector is an important part of the framework because the anomaly analysis is performed only on the detected objects (regions). Thus, if the object detector fails to detect an object of interest (anomalous), the framework will completely miss the respective anomalous event. In the original SSMTL framework, the YOLOv3 [60] object detector was employed. Our first update is to consider the YOLOv5 [31] detector, which is known to outperform YOLOv3. Even though YOLOv5 is supposed to detect the objects more accurately than its previous versions, *e.g.* YOLOv3, an object detector can only detect a predefined set of classes. However, the set of object classes that can generate an anomaly should not be limited to a fixed number of classes, otherwise we might encounter a frame with objects which the object detector is unable to detect, *e.g.* a tree that falls on the street, blocking the traffic. Another limitation of object detectors is the inability of detecting objects affected by severe motion blur. However, fast moving objects, *e.g.* a person running, are very likely to cause an anomaly. Due to these limitations, the SSMTL framework can miss such anomalous objects. To alleviate these issues, we propose to detect objects using optical flow or background subtraction, in conjunction with a pre-trained object detector.

On the one hand, we propose to detect new objects belonging to unknown object classes or that are affected by motion blur by applying optical flow. For each frame, we compute the optical flow map with the method proposed by Liu *et al.* [39]. We consider that a pixel from the optical flow map is part of a moving object if its magnitude is larger than a threshold. Additionally, we use the YOLO bounding boxes to blackout regions of already detected objects. The resulting connected components are added to the set of detected objects. To eliminate very small objects created by the noise in the optical flow map, we impose a restriction for the width and height of each new object detected through optical flow.

On the other hand, we propose to use background subtraction as a faster alternative to optical flow. We employ a fast and intuitive approach that starts by converting the RGB frames to grayscale. We compute an initial background image for each scene by averaging several consecutive frames. We continuously update the background

throughout the video sequence. We subtract the background image from each frame to obtain the foreground objects. Then, we apply a threshold to separate the foreground pixels from the background pixels and cleaned up the result with a morphological closing operation. As for the optical flow maps, we blackout the regions already detected by YOLO and add the connected components with an area higher than a certain threshold as new objects.

3.2. Introducing New Backbones

We extend the original 3D CNN backbone of the SSMTL architecture and introduce a CvT [74] module formed of multiple sequential transformer blocks. We study two approaches of applying the transformer before and after the global temporal pooling layer, effectively modeling the input as either 2D or 3D. Hence, we name the two approaches 2D CvT and 3D CvT. For the 2D CvT module, we apply average pooling across time to obtain a 2D input of 8×8 tokens, before introducing the module. For the 3D CvT module, we first apply the module directly on the output of the shared 3D CNN backbone, the input for the CvT module having $7 \times 8 \times 8$ tokens. To make it compatible, we replace the 2D depthwise convolutions from CvT with 3D depthwise convolutions. The output of the 3D CvT module is passed through a global temporal pooling layer, producing the final output. The number of transformer blocks as well as the number of attention heads are decided according to the number of proxy tasks, based on a set of preliminary experiments discussed in Section 4.3.

3.3. Introducing New Proxy Tasks

Aside from the existing four tasks, we propose a new set of five proxy tasks, as described below. We note that the prediction and decoding heads used for the new tasks are identical to those used for the original four tasks.

T₅: Pseudo-anomalies. For the *pseudo-anomalies* task (T_5), we employ an adversarial training procedure based on gradient ascent through our shared backbone. We attach a decoder to our shared encoder which learns to reproduce images from an out-of-distribution data set formed of flowers [50], textures [34], and ImageNet [63] classes that do not appear in urban surveillance videos. We optimize the decoder using gradient descent, as usual. However, the shared backbone is optimized to model pseudo-anomalies poorly, that is, when updating the network, we reverse the sign of the learning rate for pseudo-anomalies. This design incentivizes the network to model general patterns poorly, directing the model towards overfitting the provided normal data.

T₆: Inpainting. For the *inpainting* task, our network is tasked with reconstructing a 64×64 single-frame input, out of which, a random patch is cropped out. At test time, for a given input, this procedure is repeated three times in a row, with the output of the previous step serving as input for the current one. At each step, a different random patch

is masked out. Finally, we employ the L_2 distance between the original image and the final reconstruction to estimate the anomaly level.

T₇: Segmentation. We pose the *segmentation* task as a knowledge distillation task, where the teacher is a pre-trained Mask R-CNN [24] and the student is our model. For this task, we attach a decoder to predict the segmentation map. We employ the L_2 loss between the predicted map and the ground-truth map to train our student. We use only the middle crop in the temporal sequence as input.

T₈: Jigsaw. For the *jigsaw* task, we split each input image into 4×4 patches (puzzle pieces) of 16×16 pixels each and apply a random shuffle of the patches, out of 100 predefined shuffles. We then task the network to predict the applied shuffle in a multi-way classification setting, using softmax. Let p_i be the probability predicted by the jigsaw head for the correct class. The anomaly score is given by $1 - p_i$.

T₉: Pose estimation. As for the segmentation task, we consider pose estimation as a knowledge distillation task and only use the middle crop in the temporal sequence as input. As teacher, we choose the pre-trained UniPose [3]. The student network is tasked with predicting heatmaps for each body joint, being optimized with the L_2 loss.

4. Experiments

4.1. Data Sets

Avenue. The Avenue [43] data set consists of 16 training videos containing only normal activity, and 21 test videos containing both normal and abnormal actions. The resolution of each frame is 360×640 pixels. The data set is annotated at the frame and pixel levels.

ShanghaiTech. The ShanghaiTech Campus [45] data set is one of the largest data sets for video anomaly detection, containing 437 videos. The training set contains 330 videos with normal actions while the test set consists of 107 videos with both normal and abnormal events. The resolution of each frame in the data set is 480×856 pixels. The ShanghaiTech data set is annotated at both frame and pixel levels.

UBnormal. The UBnormal [1] data set is a new supervised open-set benchmark containing abnormal actions in the training videos which are disjoint from the abnormal actions from the test videos. The entire data set has a total of 543 videos which are divided into 268 training videos, 64 validation videos and 211 test videos. The resolution of the frames can vary, the minimum side of a frame being 720 pixels. UBnormal is also annotated at both frame and pixel levels. In the experiments, we only use the normal videos to train our framework.

4.2. Evaluation and Implementation Details

Evaluation metrics. We employ the widely-used area under the curve (AUC) computed with respect to the ground-truth frame-level annotations to evaluate detection perfor-

mance. Following [1, 19, 62], we report both the micro and macro frame-level AUC scores when we compare to other state-of-the-art methods. To evaluate the localization performance of the proposed frameworks, we consider the region-based detection criterion (RBDC) and track-based detection criterion (TBDC) introduced by Ramachandra *et al.* [54]. For the preliminary experiments, we only report the more popular micro AUC measure.

Hyperparameter settings. We start from the official implementation of SSMTL¹. We keep all the original hyperparameters of the framework, established by Georgescu *et al.* [18]. For YOLOv3 and YOLOv5, we set the object detection confidence threshold to 0.8. We use a pre-trained SelfFlow [39] model to detect objects in motion, forming the objects out of pixels with a motion magnitude higher than 1. For the SelfFlow [39] and background subtraction methods, we eliminate all objects with an area smaller than 1500 pixels. As Georgescu *et al.* [18], we use temporal sequences of length 7, resulting in input tensors of $7 \times 64 \times 64 \times 3$ components. Since we remove task T_4 in our final framework configurations (SSMTL++v1/v2), we eliminate the hyperparameter λ from the original framework, using equal weights for all the remaining proxy tasks.

All models are optimized for 20 epochs using Adam [33] with a learning rate of $\eta = 10^{-3}$, keeping the default values for the other hyperparameters of Adam. Depending on the capacity of the backbone architecture, we train the models on mini-batches of 64, 128 or 256 samples. We keep 15% of the training data for validation and choose the model with the lowest validation error on the proxy tasks to be employed on the target task (anomaly detection).

There are some additional hyperparameters for the new proxy tasks added to the model. For the adversarial training with pseudo-anomalies (T_5), we adjust the adversarial learning rate to $-0.2 \cdot \eta$, thus maximizing the loss when an adversarial example is given as input. For the inpainting task (T_6), we generate mask patches of random sizes between 4 and 32 pixels. The center of each patch is generated using a 2D Gaussian distribution centered in the middle of input image, having a standard deviation of 20 in each direction.

4.3. Preliminary Experiments

Experimenting with new detection methods. We first experiment with various detection methods, presenting the results on the Avenue data set in Table 1. To evaluate each detector, we report the total number of detections in the test set together with the recall calculated with respect to the ground-truth annotations provided in [54]. Since only the anomalies are annotated, there is no way to compute precision. The optical flow adds a few additional detections for a better recall, while background subtraction adds the most

Detection Approach	#Objects	Recall	AUC
YOLOv3	111k	88.2%	83.5%
YOLOv3 + Optical Flow	113k	91.3%	89.6%
YOLOv3 + Background	118k	94.8%	88.4%
YOLOv5	105k	87.7%	86.9%
YOLOv5 + Optical Flow	110k	90.9%	89.0%
YOLOv5 + Background	120k	96.1%	88.2%

Table 1. Results (in terms of recall and frame-level micro AUC) on Avenue while varying the object detection methods of a framework trained on task T_3 (middle bounding box prediction).

Tasks	Backbone	AUC
T_3	3D CNN	89.6%
T_3	3D CNN + 2D CvT	90.1%
T_3	3D CNN + 3D CvT	90.6%
$T_1+T_2+T_3$	3D CNN	90.7%
$T_1+T_2+T_3$	3D CNN + 3D CvT	92.5%

Table 2. Results (in terms of the frame-level micro AUC) on Avenue while changing the backbone architecture for a model trained either on one task (T_3 – middle bounding box prediction) or three tasks (T_1 – arrow of time, T_2 – motion irregularity, T_3 – middle bounding box prediction).

detections, leading to the highest recall score. However, the AUC is more important. The original SSMTL framework uses the YOLOv3 detector, which leads to a micro AUC of 83.5%. YOLOv5 seems to output better object detections, providing a performance gain of 3.4%. When we add optical flow detections, the performance increases by significant margins for both YOLOv3 and YOLOv5. Interestingly, there seems to be a much higher gain by combining YOLOv3 and optical flow detections. When we introduce the detections obtained via background subtraction, we again observe considerable performance gains, but not as high as compared to optical flow. This is caused by some of the added detections being labeled as anomalies by mistake, generating a higher false positive rate. Hence, we conclude that optical flow is a better choice than background subtraction. Since the combination of YOLOv3 and optical flow gives the best micro AUC (89.6%), we continue with this detection approach in the subsequent experiments.

Experimenting with new backbones. In our second experiment, we study the effect of changing the backbone architecture from a pure 3D CNN to one based on transformer blocks. For this empirical study, we select only one task (middle bounding box reconstruction) and perform the experiments on the Avenue data set. We report the corresponding results in the first three rows of Table 2. Since the model learns only one task, we choose the shallow and narrow [18] configuration for the 3D CNN. By introducing 2D CvT blocks after performing average pooling across time, we observe a gain of 0.5% in terms of the micro AUC. We notice a higher gain (1%) upon introducing the 3D transformer module prior to the pooling across time. We keep

¹<https://github.com/lilygeorgescu/AED-SSMTL>

Blocks	Heads		
	6	12	18
1	91.6%	90.1%	91.4%
2	92.4%	92.0%	90.5%
3	91.1%	92.5%	92.2%

Table 3. Results (in terms of the frame-level micro AUC) on Avenue while varying the number of transformer blocks (from 1 to 3) and the number of attention heads (from 6 to 18). All models are trained on three tasks: T_1 (arrow of time), T_2 (motion irregularity), T_3 (middle bounding box prediction).

Tasks	Backbone	AUC
$T_1+T_2+T_3$	shared	92.5%
$T_1+T_2+T_3+T_4$	shared	92.0%
$T_1+T_2+T_3+T_5$	shared	93.7%
$T_1+T_2+T_3+T_6$	shared	91.6%
$T_1+T_2+T_3+T_7$	shared	90.7%
$T_1+T_2+T_3+T_8$	shared	90.2%
$T_1+T_2+T_3+T_9$	shared	91.1%
$T_1+T_2+T_3+T_4+T_5$	shared	89.8%
$T_1+T_2+T_3+T_4+T_6$	shared	89.5%
$T_1+T_2+T_3+T_5+T_6$	shared	90.1%
$T_1+T_2+T_3+T_4+T_5+T_6$	shared	89.6%
$T_1+T_2+T_3+T_4+T_5+T_6$	separate	90.5%

Table 4. Results (in terms of the frame-level micro AUC) on Avenue while changing the proxy tasks for a model based on the 3D CNN + 3D CvT architecture.

this backbone in the following experiments.

Next, we aim to determine if the performance gains brought by the new transformer-based backbone are consistent when introducing more tasks. We underline that for the original backbone, Georgescu *et al.* [18] increased the depth and width of the architecture along with the number of tasks. In a similar manner, we study how the number of transformer blocks (from 1 to 3) and the number of attention heads (from 6 to 18) influences the performance of the framework when we switch from one task (middle bounding box prediction) to the following three tasks: T_1 (arrow of time), T_2 (motion irregularity), T_3 (middle bounding box prediction). We present the results with various depths and widths on Avenue in Table 3. The empirical results indicate that the best configuration is to use 3 blocks with 12 attention heads each. Upon finding the optimal architecture in the context of multi-task learning, we now compare the deep+wide 3D CNN with the new backbone based on 3D CNN + 3D CvT with 3 blocks and 12 attention heads. Both models are trained on the first three tasks for a fair comparison. We report the corresponding results in the last two rows of Table 2. We observe that introducing more tasks increases the gap between the old and new backbones, by up to 1.8%. We keep the configuration based on 3 blocks and 12 attention heads for the remaining experiments.

Experimenting with new tasks. In Table 4, we present results with various task combinations on Avenue. First,

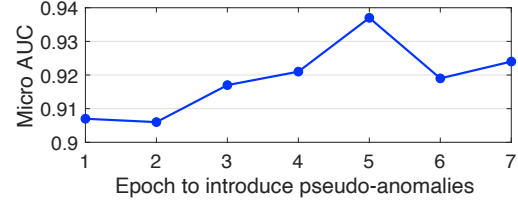


Figure 1. Frame-level AUC scores showing the effect of introducing pseudo-anomalies at different epochs while training SSMTL++v1 on Avenue.

we underline that the knowledge distillation task (T_4) from the original framework is not immediately compatible with the addition of detections based on optical flow or background subtraction, since these detections do not have an assigned object class, unlike the YOLOv3 detections. Moreover, assigning classes to these detections is not trivial as they sometimes include a single object part or multiple objects. To this end, the experiments conducted so far do not include task T_4 . However, we can introduce a new class of objects that comprises all the optical flow detections. As shown in Table 4, this solution is suboptimal, leading to a slight performance drop from 92.5% to 92.0%.

Next, we experiment with independently adding our new proxy tasks to the first three tasks, to assess the impact of each new proxy task on the performance of the whole framework. Among the new proxy tasks, we find tasks T_5 (pseudo-anomalies) and T_6 (inpainting) as the most promising. We note that task T_5 is not introduced right from the beginning, as the network needs some time to converge on the other tasks before adversarial training is enabled. As confirmed by Figure 1, it is worth waiting for a few epochs before enabling task T_5 , the optimal starting point being epoch 5.

We next attempt to combine 5 or 6 proxy tasks together, considering the most promising options. However, the results indicate significant performance drops when jointly optimizing the framework on 5 or more tasks. Our first assumption for explaining the lower results is that the backbone needs a higher capacity to cope with the larger number of tasks. We tried to increase its capacity, without obtaining any performance gains. We also tried to use a separate backbone for each task, which seems to be somewhat useful, but not enough to surpass our best performing combination of tasks (T_1, T_2, T_3 and T_5).

For the final comparison with the existing state-of-the-art methods, we choose two of our most promising models. Our first combination of tasks (SSMTL++v1) is formed of tasks T_1, T_2, T_3 and T_5 . Our second combination of tasks (SSMTL++v2) is formed of tasks T_1, T_2, T_3 and T_6 . We recall that both SSMTL++v1 and SSMTL++v2 use a hybrid detection method based on YOLOv3 and optical flow, as well as an enhanced backbone (3D CNN + 3D CvT).

Year	Method	AUC		RBDC	TBDC
		Micro	Macro		
2019	Gong <i>et al.</i> [20]	83.3	-	-	-
	Ionescu <i>et al.</i> [27]	87.4	90.4	15.8	27.0
	Ionescu <i>et al.</i> [29]	88.9	-	-	-
	Lee <i>et al.</i> [35]	90.0	-	-	-
	Nguyen <i>et al.</i> [49]	86.9	-	-	-
	Vu <i>et al.</i> [72]	71.5	-	-	-
	Wu <i>et al.</i> [75]	86.6	-	-	-
2020	Dong <i>et al.</i> [11]	84.9	-	-	-
	Doshi <i>et al.</i> [12, 13]	86.4	-	-	-
	Ji <i>et al.</i> [30]	78.3	-	-	-
	Lu <i>et al.</i> [44]	85.8	-	-	-
	Park <i>et al.</i> [52]	88.5	-	-	-
	Ramachandra <i>et al.</i> [54]	72.0	-	35.8	80.9
	Ramachandra <i>et al.</i> [55]	87.2	-	41.2	78.6
	Sun <i>et al.</i> [68]	89.6	-	-	-
	Wang <i>et al.</i> [73]	87.0	-	-	-
	Yu <i>et al.</i> [81]	89.6	-	-	-
2021	Astrid <i>et al.</i> [4]	84.9	-	-	-
	Astrid <i>et al.</i> [5]	87.1	-	-	-
	Chang <i>et al.</i> [7]	87.1	-	-	-
	Georgescu <i>et al.</i> [19]	92.3	90.4	65.1	66.9
	Madan <i>et al.</i> [46]	88.6	-	-	-
	Li <i>et al.</i> [36]	88.8	-	-	-
	Liu <i>et al.</i> [42]	91.1	93.5	41.1	86.2
	Yang <i>et al.</i> [79]	88.6	-	-	-
	Yu <i>et al.</i> [82]	90.2	-	-	-
	SSMTL [18]	91.5	91.9	57.0	58.3
2022	Georgescu <i>et al.</i> [19]+SSPCAB [62]	92.9	91.9	66.0	64.9
	Lin <i>et al.</i> [38]	90.3	-	-	-
	Liu <i>et al.</i> [40]+SSPCAB [62]	87.3	84.5	20.1	62.3
	Liu <i>et al.</i> [42]+SSPCAB [62]	90.9	92.2	62.3	89.3
	Park <i>et al.</i> [51]	85.3	-	-	-
	Yu <i>et al.</i> [80]	92.8	-	-	-
	SSMTL++v1 (ours)	93.7	91.7	40.9	82.1
	SSMTL++v2 (ours)	91.6	92.5	47.8	85.2

Table 5. Comparison of the proposed frameworks (SSMTL++v1 and SSMTL++v2) with the original SSMTL [19] as well as other state-of-the-art methods on the Avenue data set. The top three scores for each metric are highlighted in **red bold** (top method), **green** (second best) and **blue** (third best).

4.4. Comparison with State of the Art

Results on Avenue. We present the comparative results of SSMTL++v1 and SSMTL++v2 versus the state-of-the-art methods on the Avenue data set in Table 5. Compared to SSMTL, we observe that SSMTL++v1 and SSMTL++v2 attain better micro AUC, macro AUC and TBDC scores, but the new models register drops in terms of RBDC. The high gains (+23.8% and +26.9%) in terms of TBDC are caused by introducing the new detections obtained by optical flow, which generate longer and consistent object tracks. Unfortunately, some of the new object detections are labeled as anomalous by mistake, increasing the false positive

Year	Method	AUC		RBDC	TBDC
		Micro	Macro		
2019	Gong <i>et al.</i> [20]	71.2	-	-	-
	Ionescu <i>et al.</i> [27]	78.7	84.9	20.7	44.5
	Lee <i>et al.</i> [35]	76.2	-	-	-
2020	Dong <i>et al.</i> [11]	73.7	-	-	-
	Doshi <i>et al.</i> [12, 13]	71.6	-	-	-
	Lu <i>et al.</i> [44]	77.9	-	-	-
	Park <i>et al.</i> [52]	70.5	-	-	-
	Sun <i>et al.</i> [68]	74.7	-	-	-
	Wang <i>et al.</i> [73]	79.3	-	-	-
2021	Yu <i>et al.</i> [81]	74.8	-	-	-
	Astrid <i>et al.</i> [4]	76.0	-	-	-
	Astrid <i>et al.</i> [5]	73.7	-	-	-
	Chang <i>et al.</i> [7]	73.7	-	-	-
	Georgescu <i>et al.</i> [19]	82.7	89.3	41.3	78.8
	Madan <i>et al.</i> [46]	74.6	-	-	-
	Li <i>et al.</i> [36]	73.9	-	-	-
	Liu <i>et al.</i> [42]	76.2	-	-	-
	Yang <i>et al.</i> [79]	74.5	-	-	-
	SSMTL [18]	82.4	89.3	42.8	83.9
2022	Georgescu <i>et al.</i> [19]+SSPCAB [62]	83.6	89.5	40.6	83.5
	Liu <i>et al.</i> [40]+SSPCAB [62]	74.5	82.9	18.5	60.2
	Liu <i>et al.</i> [42]+SSPCAB [62]	75.5	83.7	45.5	84.5
	Park <i>et al.</i> [51]	72.2	-	-	-
	Yu <i>et al.</i> [80]	72.1	-	-	-
	Zaheer <i>et al.</i> [84]	79.6	-	-	-
	SSMTL++v1 (ours)	82.9	89.8	43.2	84.1
	SSMTL++v2 (ours)	83.8	90.5	47.1	85.6

Table 6. Comparison of the proposed frameworks (SSMTL++v1 and SSMTL++v2) with the original SSMTL [19] as well as other state-of-the-art methods on the ShanghaiTech data set. The top three scores for each metric are highlighted in **red bold** (top method), **green** (second best) and **blue** (third best).

rate and causing important drops in terms of RBDC. However, the TBDC gains outweigh the RBDC drops. Moreover, SSMTL++v1 attains the highest micro AUC (93.7%) among all models.

Results on ShanghaiTech. We present the results of the comparative study conducted on ShanghaiTech in Table 6. We observe that both SSMTL++v1 and SSMTL++v2 obtain consistent improvements over SSMTL [18] across all metrics. Remarkably, SSMTL++v2 attains the top performance on each metric, surpassing all other approaches. At the same time, SSMTL++v1 shares the second and third places (depending on the metric) with two state-of-the-art frameworks (Georgescu *et al.* [19] and Liu *et al.* [40]) which were recently enhanced with self-supervised predictive convolutional attentive blocks (SSPCAB) [62].

Results on UBnormal. As the UBnormal [1] benchmark is very new, the number of existing results is relatively small. Nevertheless, we showcase the results of the comparative study conducted on UBnormal in Table 7. As for

Method	AUC		RBDC	TBDC
	Micro	Macro		
Sultani <i>et al.</i> [67] (pre-trained)	49.5	77.4	< 0.01	< 0.01
Sultani <i>et al.</i> [67] (fine-tuned)	50.3	76.8	< 0.01	< 0.01
Bertasius <i>et al.</i> [6] (1/32 rate)	68.5	80.3	0.04	0.05
Bertasius <i>et al.</i> [6] (1/8 rate)	64.1	75.4	0.04	0.05
Bertasius <i>et al.</i> [6] (1/4 rate)	61.9	75.4	0.04	0.06
Georgescu <i>et al.</i> [19]	59.3	84.9	21.91	53.44
Georgescu <i>et al.</i> [19]+UBnormal	61.3	85.6	25.43	56.27
SSMTL [18]	55.4	84.5	19.71	55.80
SSMTL++v1 (ours)	62.1	86.5	25.63	63.53
SSMTL++v2 (ours)	56.0	85.9	20.33	57.76

Table 7. Comparison of the proposed frameworks (SSMTL++v1 and SSMTL++v2) with the original SSMTL [19] as well as other state-of-the-art methods on the UBnormal data set. The top three scores for each metric are highlighted in **red bold** (top method), **green** (second best) and **blue** (third best).

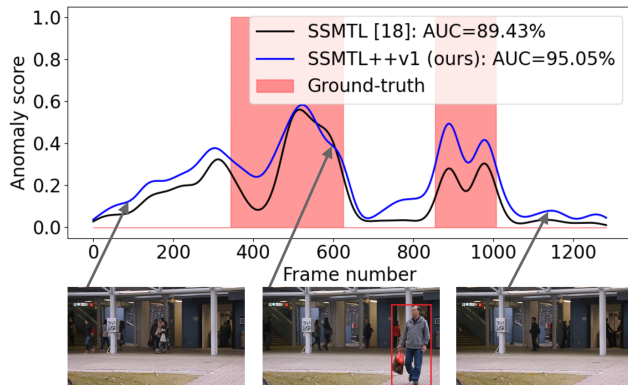


Figure 2. Comparing the anomaly scores (on the vertical axis) of SSMTL [18] and SSMTL++v1 on the frames (on the horizontal axis) from test video 06 in Avenue. Best viewed in color.

the ShanghaiTech data set, we notice that both SSMTL++v1 and SSMTL++v2 surpass the original SSMTL method. Furthermore, SSMTL++v1 establishes new state-of-the-art levels for three metrics (macro AUC, RBDC and TBDC), while SSMTL++v2 is the second best method for two of the metrics (macro AUC and TBDC). Although the TimeSformer of Bertasius *et al.* [6] seems very good at determining if a video frame is abnormal or not, the model is not able to localize anomalies. The TBDC and RBDC differences in favor of our models outweigh the lower micro AUC scores compared to TimeSformer.

Qualitative analysis. We present a few test videos to assess the quality of the predicted anomaly scores with respect to the ground-truth. In Figure 2, we observe that the AUC gains brought by SSMTL++v1 over SSMTL are higher than 5%. The person labeled as anomalous by SSMTL++v1 is walking in the wrong direction. In Figure 3, we notice that SSMTL++v2 is outperforming SSMTL by a significant margin (+14%). SSMTL++v2 labels two persons as

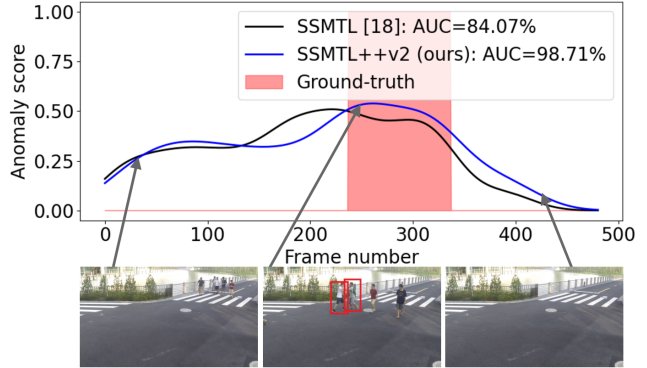


Figure 3. Comparing the anomaly scores (on the vertical axis) of SSMTL [18] and SSMTL++v2 on the frames (on the horizontal axis) from test video 07_0049 in ShanghaiTech. Best viewed in color.

anomalous because they are fighting. We present additional qualitative results in the supplementary.

Running time. We discuss the running time of SSMTL++v1 and SSMTL++v2 in the supplementary.

5. Conclusion

In this work, we revisited the self-supervised multi-task learning framework introduced in [18], proposing a series of updates that boost the performance of the original method to new state-of-the-art levels. We provided empirical evidence for several beneficial updates. First, we showed that using optical flow along with YOLOv3 to obtain object detections is very useful in finding more objects. Second, we obtained additional performance gains by integrating 3D convolutional multi-head attention blocks into the backbone architecture. Furthermore, we showed that the *adversarial training on pseudo-anomalies* and *inpainting* tasks are well-correlated to anomaly detection, leading to performance improvements of the multi-task learning pipeline. Interestingly, these new proxy tasks are useful when replacing the original knowledge distillation task (T_4), rather than being added as additional proxy tasks.

Noting that models training on more than 5 tasks seem to underperform, in future work, we aim to study more ways to learn from as many tasks as possible, which, at least in principle, should lead to even better results.

Acknowledgments

This work was supported by a grant of the Romanian Ministry of Education and Research, CNCS - UEFISCDI, project number PN-III-P2-2.1-PED-2021-0195, within PNCDI III. This work has also been funded by the Milestone Research Programme at AAU, and by SecurifAI.

References

- [1] Andra Acsintoae, Andrei Florescu, Mariana-Iuliana Georgescu, Tudor Mare, Paul Sumedrea, Radu Tudor Ionescu, Fahad Shahbaz Khan, and Mubarak Shah. Unnormal: New benchmark for supervised open-set video anomaly detection. In *Proceedings of CVPR*, pages 20143–20153, 2022.
- [2] Borislav Antic and Bjorn Ommer. Video parsing for abnormality detection. In *Proceedings of ICCV*, pages 2415–2422, 2011.
- [3] Bruno Artacho and Andreas Savakis. UniPose: Unified Human Pose Estimation in Single Images and Videos. In *Proceedings of CVPR*, pages 7035–7044, 2020.
- [4] Marcella Astrid, Muhammad Zaigham Zaheer, Jae-Yeong Lee, and Seung-Ik Lee. Learning memory-guided normality for anomaly detection. In *Proceedings of BMVC*, 2021.
- [5] Marcella Astrid, Muhammad Zaigham Zaheer, and Seung-Ik Lee. Synthetic Temporal Anomaly Guided End-to-End Video Anomaly Detection. In *Proceedings of ICCVW*, pages 207–214, 2021.
- [6] Gedas Bertasius, Heng Wang, and Lorenzo Torresani. Is Space-Time Attention All You Need for Video Understanding? In *Proceedings of ICML*, 2021.
- [7] Yunpeng Chang, Zhigang Tu, Wei Xie, Bin Luo, Shifu Zhang, Haigang Sui, and Junsong Yuan. Video anomaly detection with spatio-temporal dissociation. *Pattern Recognition*, 122:108213, 2022.
- [8] Kai-Wen Cheng, Yie-Tarng Chen, and Wen-Hsien Fang. Video anomaly detection and localization using hierarchical feature representation and Gaussian process regression. In *Proceedings of CVPR*, pages 2909–2917, 2015.
- [9] Y. Cong, J. Yuan, and J. Liu. Sparse reconstruction cost for abnormal event detection. In *Proceedings of CVPR*, pages 3449–3456, 2011.
- [10] Allison Del Giorno, J. Andrew Bagnell, and Martial Hebert. A Discriminative Framework for Anomaly Detection in Large Videos. In *Proceedings of ECCV*, pages 334–349, 2016.
- [11] Fei Dong, Yu Zhang, and Xiushan Nie. Dual Discriminator Generative Adversarial Network for Video Anomaly Detection. *IEEE Access*, 8:88170–88176, 2020.
- [12] Keval Doshi and Yasin Yilmaz. Any-Shot Sequential Anomaly Detection in Surveillance Videos. In *Proceedings of CVPRW*, pages 934–935, 2020.
- [13] Keval Doshi and Yasin Yilmaz. Continual Learning for Anomaly Detection in Surveillance Videos. In *Proceedings of CVPRW*, pages 254–255, 2020.
- [14] Alexey Dosovitskiy, Lucas Beyer, Alexander Kolesnikov, Dirk Weissenborn, Xiaohua Zhai, Thomas Unterthiner, Mostafa Dehghani, Matthias Minderer, Georg Heigold, Sylvain Gelly, et al. An image is worth 16x16 words: Transformers for image recognition at scale. In *Proceedings of ICLR*, 2021.
- [15] Jayanta K. Dutta and Bonny Banerjee. Online Detection of Abnormal Events Using Incremental Coding Length. In *Proceedings of AAAI*, pages 3755–3761, 2015.
- [16] Jia-Chang Feng, Fa-Ting Hong, and Wei-Shi Zheng. MIST: Multiple Instance Self-Training Framework for Video Anomaly Detection. In *Proceedings of CVPR*, pages 14009–14018, 2021.
- [17] Yachuang Feng, Yuan Yuan, and Xiaoqiang Lu. Learning deep event models for crowd anomaly detection. *Neurocomputing*, 219:548–556, 2017.
- [18] Mariana-Iuliana Georgescu, Antonio Barbalau, Radu Tudor Ionescu, Fahad Shahbaz Khan, Marius Popescu, and Mubarak Shah. Anomaly Detection in Video via Self-Supervised and Multi-Task Learning. In *Proceedings of CVPR*, pages 12742–12752, 2021.
- [19] Mariana Iuliana Georgescu, Radu Ionescu, Fahad Shahbaz Khan, Marius Popescu, and Mubarak Shah. A Background-Agnostic Framework with Adversarial Training for Abnormal Event Detection in Video. *IEEE Transactions on Pattern Analysis and Machine Intelligence*, 2021.
- [20] Dong Gong, Lingqiao Liu, Vuong Le, Budhaditya Saha, Moussa Reda Mansour, Svetha Venkatesh, and Anton Van Den Hengel. Memorizing Normality to Detect Anomaly: Memory-Augmented Deep Autoencoder for Unsupervised Anomaly Detection. In *Proceedings of ICCV*, pages 1705–1714, 2019.
- [21] Mahmudul Hasan, Jonghyun Choi, Jan Neumann, Amit K. Roy-Chowdhury, and Larry S. Davis. Learning temporal regularity in video sequences. In *Proceedings of CVPR*, pages 733–742, 2016.
- [22] Kaiming He, Xinlei Chen, Saining Xie, Yanghao Li, Piotr Dollár, and Ross Girshick. Masked autoencoders are scalable vision learners. In *Proceedings of the IEEE/CVF Conference on Computer Vision and Pattern Recognition*, pages 16000–16009, 2022.
- [23] Kaiming He, Haoqi Fan, Yuxin Wu, Saining Xie, and Ross Girshick. Momentum contrast for unsupervised visual representation learning. In *Proceedings of the IEEE/CVF conference on computer vision and pattern recognition*, pages 9729–9738, 2020.
- [24] Kaiming He, Georgia Gkioxari, Piotr Dollar, and Ross Girshick. Mask R-CNN. In *Proceedings of ICCV*, pages 2980–2988, 2017.
- [25] Kaiming He, Xiangyu Zhang, Shaoqing Ren, and Jian Sun. Deep Residual Learning for Image Recognition. In *Proceedings of CVPR*, pages 770–778, 2016.
- [26] Ryota Hinami, Tao Mei, and Shin’ichi Satoh. Joint Detection and Recounting of Abnormal Events by Learning Deep Generic Knowledge. In *Proceedings of ICCV*, pages 3639–3647, 2017.
- [27] Radu Tudor Ionescu, Fahad Shahbaz Khan, Mariana-Iuliana Georgescu, and Ling Shao. Object-Centric Auto-Encoders and Dummy Anomalies for Abnormal Event Detection in Video. In *Proceedings of CVPR*, pages 7842–7851, 2019.
- [28] Radu Tudor Ionescu, Sorina Smeureanu, Bogdan Alexe, and Marius Popescu. Unmasking the abnormal events in video. In *Proceedings of ICCV*, pages 2895–2903, 2017.
- [29] Radu Tudor Ionescu, Sorina Smeureanu, Marius Popescu, and Bogdan Alexe. Detecting abnormal events in video using Narrowed Normality Clusters. In *Proceedings of WACV*, pages 1951–1960, 2019.

- [30] Xiangli Ji, Bairong Li, and Yuesheng Zhu. TAM-Net: Temporal Enhanced Appearance-to-Motion Generative Network for Video Anomaly Detection. In *Proceedings of IJCNN*, pages 1–8, 2020.
- [31] Glenn Jocher, Ayush Chaurasia, Alex Stoken, Jirka Borovec, Yonghye Kwon, et al. ultralytics/yolov5: v6.1 - TensorRT, TensorFlow Edge TPU and OpenVINO Export and Inference, 2022.
- [32] Jaechul Kim and Kristen Grauman. Observe locally, infer globally: A space-time MRF for detecting abnormal activities with incremental updates. In *Proceedings of CVPR*, pages 2921–2928, 2009.
- [33] Diederik P. Kingma and Jimmy Ba. Adam: A method for stochastic optimization. In *Proceedings of ICLR*, 2015.
- [34] Svetlana Lazebnik, Cordelia Schmid, and Jean Ponce. A Sparse Texture Representation Using Local Affine Regions. *IEEE Transactions on Pattern Analysis and Machine Intelligence*, 27(8):1265–1278, 2005.
- [35] Sangmin Lee, Hak Gu Kim, and Yong Man Ro. BMAN: Bidirectional Multi-Scale Aggregation Networks for Abnormal Event Detection. *IEEE Transactions on Image Processing*, 29:2395–2408, 2019.
- [36] Bo Li, Sam Leroux, and Pieter Simoens. Decoupled appearance and motion learning for efficient anomaly detection in surveillance video. *Computer Vision and Image Understanding*, 210:103249, 2021.
- [37] Weixin Li, Vijay Mahadevan, and Nuno Vasconcelos. Anomaly detection and localization in crowded scenes. *IEEE Transactions on Pattern Analysis and Machine Intelligence*, 36(1):18–32, 2014.
- [38] Xiangru Lin, Yuyang Chen, Guanbin Li, and Yizhou Yu. A Causal Inference Look at Unsupervised Video Anomaly Detection. In *Proceedings of AAAI*, pages 1620–1629, 2022.
- [39] Pengpeng Liu, Michael R. Lyu, Irwin King, and Jia Xu. SelfFlow: Self-Supervised Learning of Optical Flow. In *Proceedings of CVPR*, pages 4571–4580, 2019.
- [40] Wen Liu, Weixin Luo, Dongze Lian, and Shenghua Gao. Future Frame Prediction for Anomaly Detection – A New Baseline. In *Proceedings of CVPR*, pages 6536–6545, 2018.
- [41] Yusha Liu, Chun-Liang Li, and Barnabás Póczos. Classifier Two-Sample Test for Video Anomaly Detections. In *Proceedings of BMVC*, 2018.
- [42] Zhian Liu, Yongwei Nie, Chengjiang Long, Qing Zhang, and Guiqing Li. A Hybrid Video Anomaly Detection Framework via Memory-Augmented Flow Reconstruction and Flow-Guided Frame Prediction. In *Proceedings of ICCV*, pages 13588–13597, 2021.
- [43] C. Lu, J. Shi, and J. Jia. Abnormal Event Detection at 150 FPS in MATLAB. In *Proceedings of ICCV*, pages 2720–2727, 2013.
- [44] Yiwei Lu, Frank Yu, Mahesh Kumar, Krishna Reddy, and Yang Wang. Few-Shot Scene-Adaptive Anomaly Detection. In *Proceedings of ECCV*, pages 125–141, 2020.
- [45] Weixin Luo, Wen Liu, and Shenghua Gao. A Revisit of Sparse Coding Based Anomaly Detection in Stacked RNN Framework. In *Proceedings of ICCV*, pages 341–349, 2017.
- [46] Neelu Madan, Arya Farkhondeh, Kamal Nasrollahi, Sergio Escalera, and Thomas B. Moeslund. Temporal Cues From Socially Unacceptable Trajectories for Anomaly Detection. In *Proceedings of ICCVW*, pages 2150–2158, 2021.
- [47] Vijay Mahadevan, Wei-Xin Li, Viral Bhalodia, and Nuno Vasconcelos. Anomaly Detection in Crowded Scenes. In *Proceedings of CVPR*, pages 1975–1981, 2010.
- [48] Ramin Mehran, Alexis Oyama, and Mubarak Shah. Abnormal crowd behavior detection using social force model. In *Proceedings of CVPR*, pages 935–942, 2009.
- [49] Trong-Nguyen Nguyen and Jean Meunier. Anomaly detection in video sequence with appearance-motion correspondence. In *Proceedings of ICCV*, 2019.
- [50] Maria-Elena Nilsback and Andrew Zisserman. A Visual Vocabulary for Flower Classification. In *Proceedings of CVPR*, pages 1447–1454, 2006.
- [51] Chaewon Park, MyeongAh Cho, Minhyeok Lee, and Sangyoun Lee. FastAno: Fast Anomaly Detection via Spatio-Temporal Patch Transformation. In *Proceedings of WACV*, pages 2249–2259, 2022.
- [52] Hyunjong Park, Jongyoun Noh, and Bumsub Ham. Learning Memory-guided Normality for Anomaly Detection. In *Proceedings of CVPR*, pages 14372–14381, 2020.
- [53] Didik Purwanto, Yie-Tarng Chen, and Wen-Hsien Fang. Dance With Self-Attention: A New Look of Conditional Random Fields on Anomaly Detection in Videos. In *Proceedings of ICCV*, pages 173–183, 2021.
- [54] Bharathkumar Ramachandra and Michael Jones. Street Scene: A new dataset and evaluation protocol for video anomaly detection. In *Proceedings of WACV*, pages 2569–2578, 2020.
- [55] Bharathkumar Ramachandra, Michael Jones, and Ranga Vatsavai. Learning a distance function with a Siamese network to localize anomalies in videos. In *Proceedings of WACV*, pages 2598–2607, 2020.
- [56] Bharathkumar Ramachandra, Michael Jones, and Ranga Raju Vatsavai. Perceptual metric learning for video anomaly detection. *Machine Vision and Applications*, 32:1432–1769, 2021.
- [57] Bharathkumar Ramachandra, Michael J. Jones, and Ranga Raju Vatsavai. A Survey of Single-Scene Video Anomaly Detection. *IEEE Transactions on Pattern Analysis and Machine Intelligence*, 2020.
- [58] Mahdyar Ravanbakhsh, Moin Nabi, Hossein Mousavi, Enver Sangineto, and Nicu Sebe. Plug-and-Play CNN for Crowd Motion Analysis: An Application in Abnormal Event Detection. In *Proceedings of WACV*, pages 1689–1698, 2018.
- [59] Mahdyar Ravanbakhsh, Moin Nabi, Enver Sangineto, Lucio Marcenaro, Carlo Regazzoni, and Nicu Sebe. Abnormal Event Detection in Videos using Generative Adversarial Nets. In *Proceedings of ICIP*, pages 1577–1581, 2017.
- [60] Joseph Redmon and Ali Farhadi. YOLOv3: An incremental improvement. *arXiv preprint arXiv:1804.02767*, 2018.
- [61] Huamin Ren, Weifeng Liu, Soren Ingvor Olsen, Sergio Escalera, and Thomas B. Moeslund. Unsupervised Behavior-Specific Dictionary Learning for Abnormal Event Detection. In *Proceedings of BMVC*, pages 28.1–28.13, 2015.

- [62] Nicolae-Catalin Ristea, Neelu Madan, Radu Tudor Ionescu, Kamal Nasrollahi, Fahad Shahbaz Khan, Thomas B. Moeslund, and Mubarak Shah. Self-supervised predictive convolutional attentive block for anomaly detection. In *Proceedings of CVPR*, pages 13576–13586, 2022.
- [63] Olga Russakovsky, Jia Deng, Hao Su, Jonathan Krause, Sanjeev Satheesh, Sean Ma, Zhiheng Huang, Andrej Karpathy, Aditya Khosla, Michael Bernstein, Alexander C. Berg, and Li Fei-Fei. ImageNet Large Scale Visual Recognition Challenge. *International Journal of Computer Vision*, 115(3):211–252, 2015.
- [64] Mohammad Sabokrou, Mohsen Fayyaz, Mahmood Fathy, and Reinhard Klette. Deep-Cascade: Cascading 3D Deep Neural Networks for Fast Anomaly Detection and Localization in Crowded Scenes. *IEEE Transactions on Image Processing*, 26(4):1992–2004, 2017.
- [65] Venkatesh Saligrama and Zhu Chen. Video anomaly detection based on local statistical aggregates. In *Proceedings of CVPR*, pages 2112–2119, 2012.
- [66] Sorina Smeureanu, Radu Tudor Ionescu, Marius Popescu, and Bogdan Alexe. Deep Appearance Features for Abnormal Behavior Detection in Video. In *Proceedings of ICIAF*, volume 10485, pages 779–789, 2017.
- [67] Waqas Sultani, Chen Chen, and Mubarak Shah. Real-World Anomaly Detection in Surveillance Videos. In *Proceedings of CVPR*, pages 6479–6488, 2018.
- [68] Che Sun, Yunde Jia, Yao Hu, and Yuwei Wu. Scene-Aware Context Reasoning for Unsupervised Abnormal Event Detection in Videos. In *Proceedings of ACMMM*, pages 184–192, 2020.
- [69] Yao Tang, Lin Zhao, Shanshan Zhang, Chen Gong, Guangyu Li, and Jian Yang. Integrating prediction and reconstruction for anomaly detection. *Pattern Recognition Letters*, 129:123–130, 2020.
- [70] Yu Tian, Guansong Pang, Yuanhong Chen, Rajvinder Singh, Johan W. Verjans, and Gustavo Carneiro. Weakly-Supervised Video Anomaly Detection With Robust Temporal Feature Magnitude Learning. In *Proceedings of ICCV*, pages 4975–4986, 2021.
- [71] Hanh T.M. Tran and David Hogg. Anomaly Detection using a Convolutional Winner-Take-All Autoencoder. In *Proceedings of BMVC*, 2017.
- [72] Hung Vu, Tu Dinh Nguyen, Trung Le, Wei Luo, and Dinh Phung. Robust Anomaly Detection in Videos Using Multi-level Representations. In *Proceedings of AAAI*, volume 33, pages 5216–5223, 2019.
- [73] Ziming Wang, Yuexian Zou, and Zeming Zhang. Cluster Attention Contrast for Video Anomaly Detection. In *Proceedings of ACMMM*, pages 2463–2471, 2020.
- [74] Haiping Wu, Bin Xiao, Noel Codella, Mengchen Liu, Xiyang Dai, Lu Yuan, and Lei Zhang. CvT: Introducing Convolutions to Vision Transformers. In *Proceedings of ICCV*, pages 22–31, 2021.
- [75] Peng Wu, Jing Liu, and Fang Shen. A Deep One-Class Neural Network for Anomalous Event Detection in Complex Scenes. *IEEE Transactions on Neural Networks and Learning Systems*, 31(7):2609–2622, 2019.
- [76] Shandong Wu, Brian E. Moore, and Mubarak Shah. Chaotic Invariants of Lagrangian Particle Trajectories for Anomaly Detection in Crowded Scenes. In *Proceedings of CVPR*, pages 2054–2060, 2010.
- [77] Dan Xu, Elisa Ricci, Yan Yan, Jingkuan Song, and Nicu Sebe. Learning Deep Representations of Appearance and Motion for Anomalous Event Detection. In *Proceedings of BMVC*, pages 8.1–8.12, 2015.
- [78] Dan Xu, Yan Yan, Elisa Ricci, and Nicu Sebe. Detecting Anomalous Events in Videos by Learning Deep Representations of Appearance and Motion. *Computer Vision and Image Understanding*, 156:117–127, 2017.
- [79] Zhiwei Yang, Jing Liu, and Peng Wu. Bidirectional retrospective generation adversarial network for anomaly detection in videos. *IEEE Access*, 9:107842–107857, 2021.
- [80] Guang Yu, Siqi Wang, Zhiping Cai, Xinwang Liu, Chuanfu Xu, and Chengkun Wu. Deep Anomaly Discovery From Unlabeled Videos via Normality Advantage and Self-Paced Refinement. In *Proceedings of CVPR*, pages 13987–13998, 2022.
- [81] Guang Yu, Siqi Wang, Zhiping Cai, En Zhu, Chuanfu Xu, Jianping Yin, and Marius Kloft. Cloze Test Helps: Effective Video Anomaly Detection via Learning to Complete Video Events. In *Proceedings of ACMMM*, pages 583–591, 2020.
- [82] Jongmin Yu, Younkwan Lee, Kin Choong Yow, Moongu Jeon, and Witold Pedrycz. Abnormal event detection and localization via adversarial event prediction. *IEEE Transactions on Neural Networks and Learning Systems*, pages 1–15, 2021.
- [83] Muhammad Zaigham Zaheer, Arif Mahmood, Marcella Astrid, and Seung-Ik Lee. CLAWS: Clustering Assisted Weakly Supervised Learning with Normalcy Suppression for Anomalous Event Detection. In *Proceedings of ECCV*, pages 358–376, 2020.
- [84] M. Zaigham Zaheer, Arif Mahmood, M. Haris Khan, Mattia Segu, Fisher Yu, and Seung-Ik Lee. Generative Cooperative Learning for Unsupervised Video Anomaly Detection. In *Proceedings of CVPR*, pages 14744–14754, 2022.
- [85] Xinfeng Zhang, Su Yang, Jiulong Zhang, and Weishan Zhang. Video Anomaly Detection and Localization using Motion-field Shape Description and Homogeneity Testing. *Pattern Recognition*, 105:107394, 2020.
- [86] Ying Zhang, Huchuan Lu, Lihe Zhang, Xiang Ruan, and Shun Sakai. Video anomaly detection based on locality sensitive hashing filters. *Pattern Recognition*, 59:302–311, 2016.
- [87] Bin Zhao, Li Fei-Fei, and Eric P. Xing. Online Detection of Unusual Events in Videos via Dynamic Sparse Coding. In *Proceedings of CVPR*, pages 3313–3320, 2011.
- [88] Jia-Xing Zhong, Nannan Li, Weijie Kong, Shan Liu, Thomas H. Li, and Ge Li. Graph Convolutional Label Noise Cleaner: Train a Plug-And-Play Action Classifier for Anomaly Detection. In *Proceedings of CVPR*, pages 1237–1246, 2019.

6. Supplementary

In the supplementary, we compare the inference time of SSMTL++v1 and SSMTL++v2 with SSMTL. We also provide additional qualitative results.

6.1. Running Time

In Table 8, we compare the inference time of SSMTL [18] with SSMTL++v1 and SSMTL++v2. Regarding the running time, our main changes from the original framework (SSMTL) [18] introduce additional processing (*i*) in the object detection phase due to optical flow, (*ii*) in the forward pass through the backbone due to the appended transformer blocks, and (*iii*) in the prediction phase of SSMTL++v2 due to the additional inpainting task (T_6), as it requires 3 passes through the model. We note that the pseudo-anomalies task (T_5) of SSMTL++v1 is only used during training, thus not having any influence on the inference time.

YOLOv3 [60], which is used by all methods, takes nearly 0.84 seconds to process a mini-batch of 64 frames, thus running at about 72 frames per second (FPS). The optical flow is obtained using the pre-trained SelfFlow [39], running at 30 FPS on mini-batches of 32 frames.

The SSMTL++v1 network processes one object-centric temporal sequence in 12 milliseconds (ms), without batching. For an object-centric approach, we can naturally batch the objects detected in each frame, resulting in a processing time of 3 ms per object-centric temporal sequence for a mini-batch size of 7 samples, corresponding to the average number of detections per frame in the Avenue test set. SSMTL++v2 processes an object-centric temporal sequence in 4 ms with an identical mini-batch size.

SSMTL can process the video frames from the Avenue test set at about 50 FPS. Due to the introduction of optical flow in the object detection phase and the deeper backbone, the inference times for SSMTL++v1 and SSMTL++v2 decrease to about 15 FPS, considering a sequential processing pipeline on a single thread. However, running SSMTL++v1 and SSMTL++v2 on two threads in parallel increases the speed to about 20 FPS, while still using a single GPU. Hence, both SSMTL++v1 and SSMTL++v2 are fast enough to process the video in real-time. The reported running times were measured on a GeForce GTX 3090 GPU with 24 GB of VRAM.

Our main bottleneck is the optical flow framework. We note that the focus of this work has been on precision in terms of anomaly detection capabilities, without much effort being dedicated towards optimizing the running time. Alternatively, faster object detectors can be applied, as well as using the faster background subtraction (55 FPS), at a small cost of precision, if inference time is a higher priority.

Method	FPS
SSMTL [18]	50.0
SSMTL++v1	20.2
SSMTL++v2	18.8

Table 8. Running time (in terms of FPS) on Avenue for SSMTL versus SSMTL++v1 and SSMTL++v2. All models are trained on four proxy tasks, thus having four prediction heads. The reported running times were measured on a GeForce GTX 3090 GPU with 24 GB of VRAM.

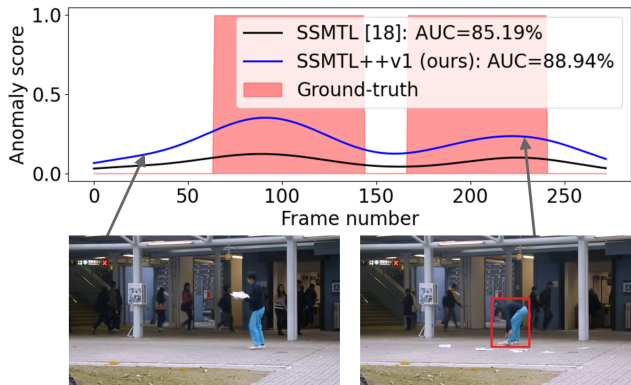


Figure 4. Comparing the anomaly scores (on the vertical axis) of SSMTL [18] and SSMTL++v1 on the frames (on the horizontal axis) from test video 20 in Avenue. Best viewed in color.

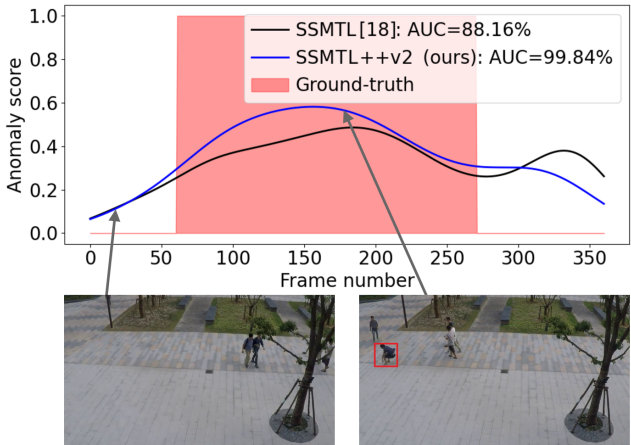


Figure 5. Comparing the anomaly scores (on the vertical axis) of SSMTL [18] and SSMTL++v2 on the frames (on the horizontal axis) from test video 04_0013 in ShanghaiTech. Best viewed in color.

6.2. More Qualitative Results

We present results for additional test videos to further analyze the quality of the predicted anomaly scores for SSMTL and SSMTL++v1/v2 with respect to the ground-truth. In Figure 4, we notice that the AUC gains brought by SSMTL++v1 over SSMTL are higher than 4%. The person labeled as anomalous by SSMTL++v1 is throwing and gathering papers on the ground. In Figure 5, we observe that SSMTL++v2 is outperforming SSMTL by a significant

margin (+11%). SSMTL seems to activate on the last 50 frames (with indexes higher than 310) in the video, producing a false positive event, while SSMTL++v2 does not trigger an anomaly for the same event. SSMTL++v2 outputs higher anomaly scores only for the person jumping, which is labeled as a true anomaly.